Beyond Larson's Law: Unveiling the Universal Structure of Molecular Clouds using Dendrogram Analysis

Author: Borja Canut Garduño
Facultat de Física, Universitat de Barcelona, Diagonal 645, 08028 Barcelona, Spain.

Advisor: Gemma Busquet Rico

Abstract: We present observations of the emission of $C^{18}O$ (1–0) and ^{13}CO (1–0) rotational lines in the southern region of the Infrared Dark Cloud G14.225–0.506. Using the dendrograms analysis, we investigate whether the substructures within the cloud obey the first Larson Law: $\sigma \propto R^{0.5}$. Identifying 1061 and 2564 structures for $C^{18}O$ and ^{13}CO respectively, we observe a well-defined correlation between velocity dispersion and size. The obtained power law indices are $\beta = 0.71$ and $\beta = 0.65$, far from the expected value of 0.5. The smallest structures present a weak relation between the magnitudes, with a lower β power law index. Comparing the results with other works from the literature covering a wide range of spatial scales we conclude that the first Larson Law seems to break at 0.01 - 0.1 pc scales.

I. INTRODUCTION

Stars form within molecular clouds. These are interstellar gas regions composed mainly of H_2 alongside less abundant molecules like CO or NH_3. These clouds typically reach extensions of $\sim$5 pc, with giant molecular clouds (GMC) exceeding these dimensions. Molecular clouds are characterized by low temperatures (10 - 30 K), densities between 10^3 and 10^5 cm^{-3} and very high masses ($M = 1000$ M$_\odot$) [1]. These clouds are not homogeneous, instead they are composed of elongated substructures (filaments) and clumps that further fragment into dense cores with sizes of 0.1 pc.

As there is no dipole moment in H_2 molecule, it is hard to study; therefore the focus is on the CO, the most abundant molecule after H_2. The CO has a small dipole moment, so the coefficient of spontaneous emission (Einstein's coefficient) of the rotational transitions is also small. At the typical temperatures and densities of molecular clouds, the lower rotational levels of CO are easily excited enabling to detect the emission [1].

Investigations of GMCs show that there are three empirical scaling relations between different magnitudes named Larson's Laws [2].

The first relation he found was between clouds size (pc) and its velocity dispersion (km s^{-1}), following $\sigma \propto \mathrm{R}^{0.38}$, interpreted as a result of interstellar turbulence. Years later, this value was modified to $\sigma \propto R^{0.5}$ by Solomon, who analysed the CO emission of 273 molecular clouds, and supported by subsequent studies [3, 4].

Second Larson's law relates the mass of the cloud (in M$_\odot$) and the velocity dispersion (km s^{-1}) with $\sigma \propto M^{0.2}$. A positive relation between the magnitudes affirm that measured structures are close to virial equilibrium [2].

Finally, third's Larson law establish a relation between the volume density (cm^{-3}) and the size (pc). The relation is $\rho \propto R^{-1.1}$ and indicates that the column density is near to be constant [2].

In this work we focus on first Larson's law by analysing different structures in the Infrared Dark Cloud (IRDC) G14.225–0.506 (hereafter G14.2). The IRDC G14.2 is part of the large cloud discovered by Elmegreen & Lada in 1976, found at the southwest of the Galactic HII region Messier 17 [5]. The distance to the cloud was obtained recently combining photometric data with *Gaia* DR2 parallax measurements [6], 1.488 - 1.574 kpc [7]. In this work we use a value of 1.6 kpc. G14.2 is formed by several filament and dense cores [8]. In this project we study the molecular lines of ^{13}CO (1–0) and $C^{18}O$ (1–0) in the southern part of the IRDC G14.2. The objective is to extract the hierarchical structure (filaments and cores) of the cloud and determine if they follow a similar relation to Larson's or Solomon's.

II. METHODOLOGY

The data analysed in this work is part of the research project 2018.1.01347.S, and has been obtained with the Atacama Large Millimeter/submillimeter Array (ALMA) [9]. The observations were made combining the main array interferometer (fifty antennas, 12-meters diameter each one) and the Atacama Compact Array (ACA; 12 antennas, 7-meter diameter each one). We have not processed this data, the images (in FITS format) of the southern part of G14.2 were provided to us. In this work we analyse the emission of the ^{13}CO (1–0) and $C^{18}O$ (1–0) rotational lines at rest frequencies of 110.2013543 GHz and 109.7821734 GHz, respectively. Frequencies were taken from The Cologne Database for Molecular Spectroscopy [10]. For both images the beam's solid angle resolution is $\sim 3''$. The background noise (rms) in both images is $\sigma_{\mathrm{rms}} = 0.012$ Jy/beam.

The images' visualization and analysis was performed via software to process the data from the ALMA telescope called Common Astronomy Software Applications (CASA) [11]. Using different CASA tasks we obtained the emission spectrum over the whole field of view and the background noise value (rms) that is important for the dendrogram's generation. We also generated images of the integrated emission (zeroth order moment map).

A. Dendrogram analysis

Dendrograms are tree-shaped diagrams of data that represent the hierarchical grouping of objects [12]. The data is grouped into sets according to their similarity and are represented as different branches of the tree. Within sets there can be subgroups of data. Branches can be divided into other structures either with branches or leaves, which are structures without any substructures. The trunk is the lowest level of the dendrogram, there can be more than one and it can be a branch or a leaf. In this project we employed the dendrogram technique on the ^{13}CO and C^{18}O data cubes using the `astrodendro` package [13] with the goal of extracting the hierarchical structure of the molecular gas to obtain the size and velocity dispersion of the different structures in the southern part of G14.2.

The generation of the dendrograms require three different parameters. A minimum value must be set to omit possible background noise, pixels below this value are not shown in the tree. Typically, this value ranges from $3\sigma_{\rm rms}$ to $6\sigma_{\rm rms}$, where $\sigma_{\rm rms}$ is the noise level of the image. Because of the noise it is necessary to set a minimum height value to consider a structure. In this case it is used a value between $1\sigma_{\rm rms}$ and $3\sigma_{\rm rms}$. Finally, it must be taken in consideration a minimum number of pixels that a structure should contain to remain an independent structure. Since the resolution of the beam is $3''$ and that of the pixel $0.5''$, this value must be at least 6 pixels. By varying these parameters, dendrograms with different number of structures are obtained.

We generated the dendrograms of the C^{18}O using different values of the three parameters. For the min_value: $3\sigma_{\rm rms}$, $4\sigma_{\rm rms}$, $5\sigma_{\rm rms}$ and $6\sigma_{\rm rms}$, for the min_delta: $\sigma_{\rm rms}$, $2\sigma_{\rm rms}$ and $3\sigma_{\rm rms}$, and for the min_npix: 12, 16, 20 and 24. Combining all this values we obtained a total of 48 dendrograms with a number of structures between 1211 and 7575. Analysing the different dendrograms we considered that most of them have to many small structures that complicate the interpretation because they do not contain information on the velocity dispersion. We chose the dendrogram with min_value = $6\sigma_{\rm rms}$, min_delta = $3\sigma_{\rm rms}$ and min_npix = 24 to minimize the number of structures. After this analysis we generated one dendrogram of ^{13}CO (2564 structures identified) and one of C^{18}O (1061 structures identified) associated only to G14.2.

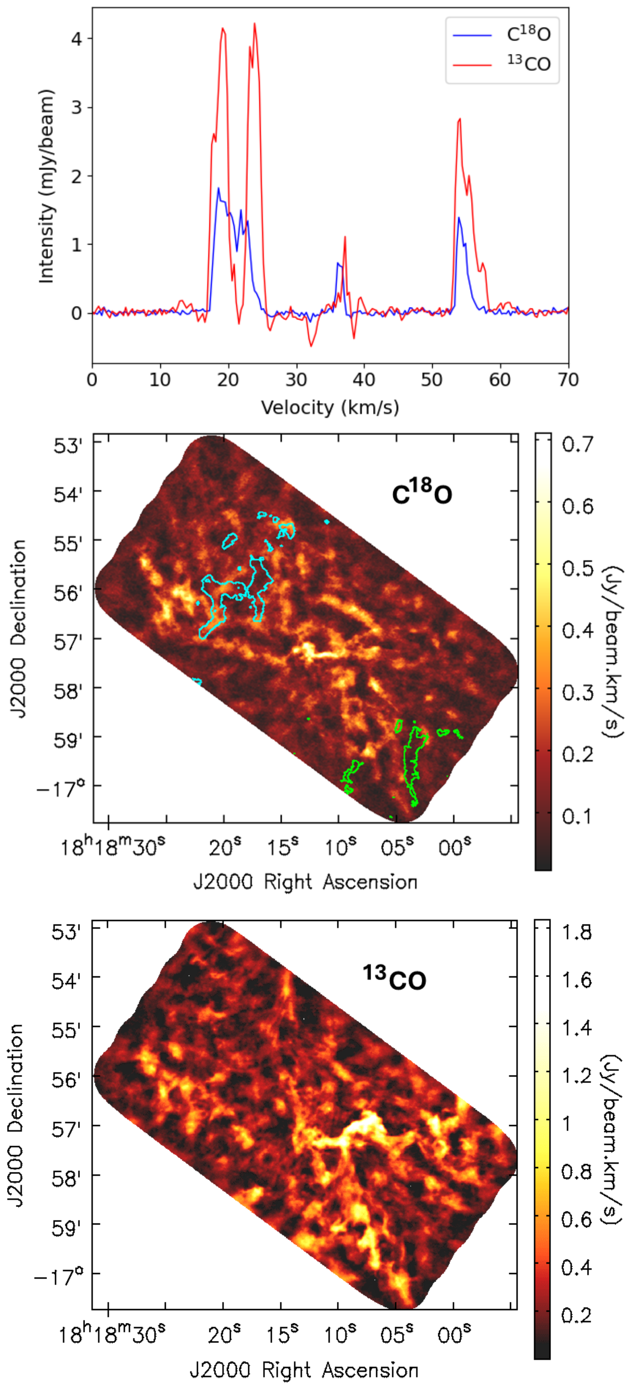

FIG. 1: *Top*: C^{18}O (1–0) and ^{13}CO (1–0) emission spectra of G14.2 southern region. *Middle*: Integrated intensity map of C^{18}O (1–0). In the color map the integration of the spectrum for 17.3 - 26.5 km s^{-1} velocities. The green and blue contour maps indicate the moment 0 in the ranges of 35.4 - 38.1 km s^{-1} and 52.6 - 57.9 km s^{-1}, respectively. *Bottom*: Integrated intensity map of ^{13}CO (1–0) between 16.9 - 25.9 km s^{-1}.

III. RESULTS

A. C^{18}O and ^{13}CO emission

Using the viewer task of CASA we present in Figure 1 (top panel) the spectrum of C^{18}O (1–0) and ^{13}CO (1–0). We can observe four emission peaks at different velocities and intensities. The first two and strongest components correspond to velocities near to 20 km s^{-1}. The

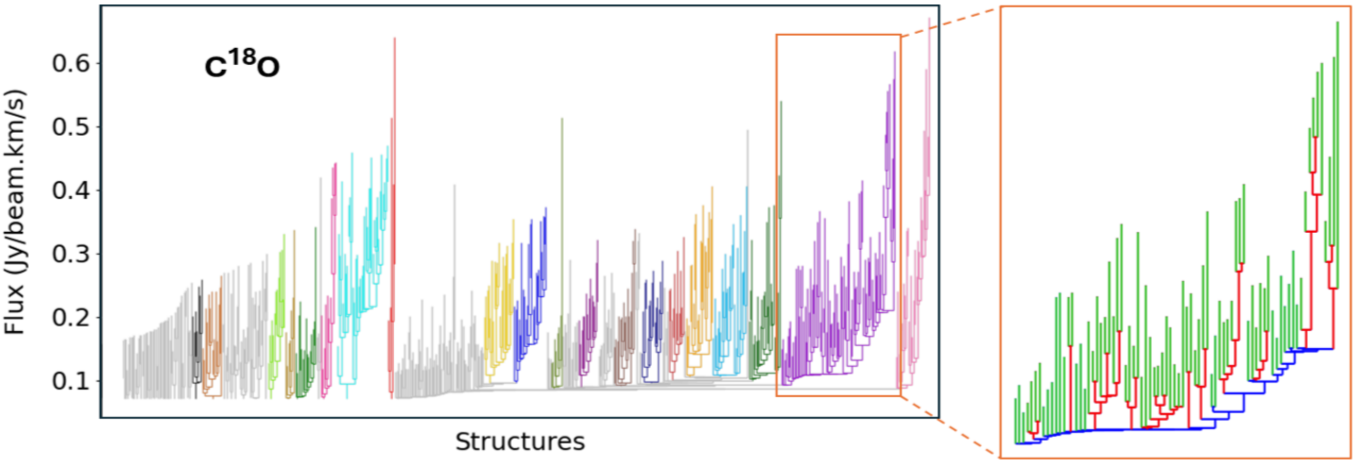

FIG. 2: *Left*: Dendrogram of C^{18}O generated with the parameters: min_value = $6\sigma_{rms}$, min_delta = $3\sigma_{rms}$ and min_pix = 24. It has a total of 1211 structures: 683 leaves and 528 branches. Of these, 117 leaves and 37 branches are trunks. In colors the more remarkable big structures. On the right there is an enlarged part of the full dendrogram where blue and red indicate subbranches and color green corresponds to the leaves.

third component is find at velocities of $\sim$37 km s^{-1} and the fourth component at $\sim$55 km s^{-1}. The main velocity components of G14.2 are in a range of 18 - 23 km s^{-1} [8]. This indicates that the last two components of the spectra correspond to emission in the same line of sight but they are not part of the IRDC G14.2. In fact, the dendrogram analysis show that these three velocity components are not related. We do not know the distance to the other structures, hence they are not included in the analysis of Larson's law. For the ^{13}CO (1–0) the separation of the first and second peaks is larger. The emission of CO molecule is very extended due to its low density, which is filtered out by the ALMA interferometer, producing the absorption signature at velocities close to the cloud's systemic velocity.

In Figure 1 (middle) we show the zero-order moment map of C^{18}O for the three velocity components seen in the spectrum. The color map indicates the emission for the G14.2 gas and the contour maps in green and blue, the emission of the third and fourth intensity peak respectively. It is also shown the color map of the integrated value of the spectrum of ^{13}CO (1–0) only for G14.2 (Figure 1-bottom). In both of the representations it is observable high density zones with filamentary morphology. Mostly, the higher emission zones for both molecules match in position although the intensity varies because the C^{18}O has a higher critical density and it is less abundant. The morphology of the gas is also consistent with the distribution of the NH_3 [8] and N_2H^+ [14] molecules.

B. Dendrograms and catalogs

In Figure 2 we can observe the C^{18}O dendrogram tree showing in some colors the different substrucutres of the cloud. It represents all the emission spectrum, including the two intensity peaks that do not belong to the IRDC G14.2. Due to the chosen parameters for the dendrogram generation, we can see a big structure coming out from a trunk representing the G14.2 and other not related structures that correspond to the other peaks. In the enlarged part of the figure we observed the hierarchy of a substructure of G14.2, showing all the leaves and branches.

We collected several properties of dendrograms structures in catalogs. The information of the catalogs we are using is the velocity dispersion (km s^{-1}) and the equivalent radius (arcsec). For the unit conversion of the size we are taking a constant distance to all the structures: 1.6 kpc. For the dendrograms associated to G14.2 we generated four catalogs for both C^{18}O and ^{13}CO: for the leaves, branches, trunks and all the structures. The ones with null velocity dispersion are not taken into consideration in the next calculus.

C. First Larson's law

We can study the relation between velocity dispersion and the equivalent radius by $\sigma = \alpha R^{\beta}$ and use the equation $\log(\sigma) = \beta \log(R) + \alpha'$ to determine the power law relation and investigate the first Larson's law.

Figure 3 shows the relation between the velocity dispersion and the size of all structures identified in C^{18}O (left) and ^{13}CO (right). The power law indices we obtained are $\beta = 0.71 \pm 0.02$ and $\beta = 0.66 \pm 0.01$, respectively. The fits for the branches have similar coefficients to the total structures of the dendrogram. These results do not follow the power law relation obtained by Solomon ($\beta = 0.5$). Even so, the correlation coefficients of these catalogs are large enough to ignore a dependency between the studied magnitudes.

Otherwise, the fit for the leaves is considerably different, obtaining lower coefficients of the relation: $\beta = 0.22$

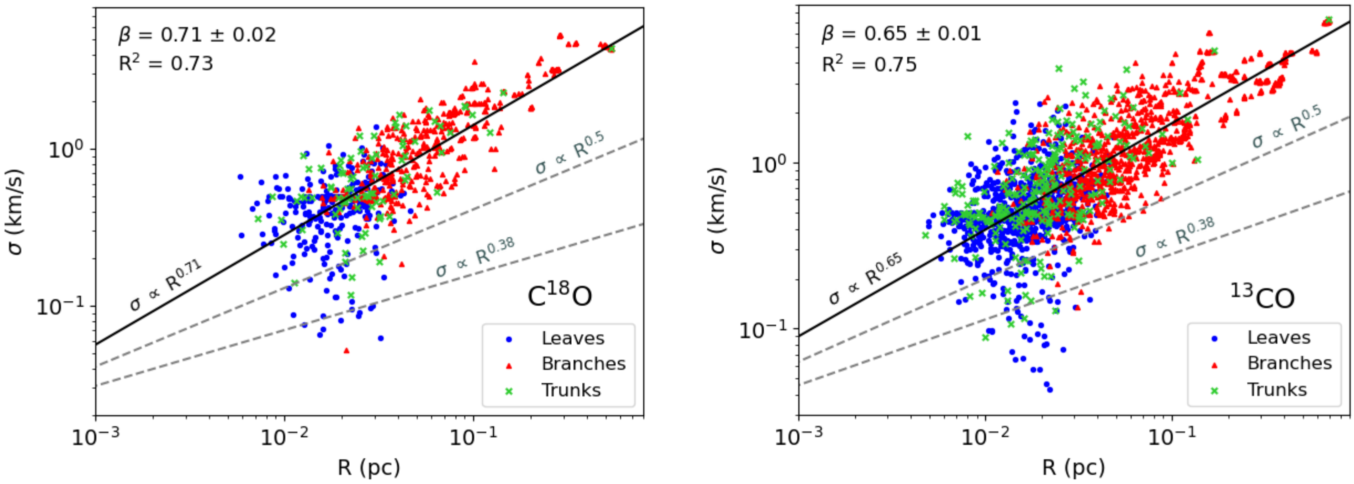

FIG. 3: Velocity dispersion as a function of the radius of dendrogram's structures for the $C^{18}O$ (1–0) (left) and the ^{13}CO (1–0) (right). Each panel shows the trend line of the regression (black line) and the Larson's and Solomon's power-laws (grey lines).

± 0.08 ($C^{18}O$) and β = 0.32 ± 0.04 (^{13}CO). We also can observe in Figure 3 some data points at lower radius (mainly leaves) that deviate of the tendency. This results are consistent with the Caselli and Myers' work (β = 0.21) [15] and with the hypothesis that $\sigma \propto R^{0.5}$ relation breaks in massive structures of molecular clouds [16]. However, the correlation coefficients are very small (see Table I), suggesting a non relation between the velocity dispersion and the size in such small structures.

The trunks' catalogs show a relation very similar to branches ones but 66% ($C^{18}O$) and 77% (^{13}CO) of the trunks of these catalogs correspond to leaves. In Table I there are the β and correlation coefficients obtained for the catalogs of the different structures we generated.

In the histograms (Figure 4) is presented the data we analysed of G14.2 as a divided quantity of first Larson's law ($\sigma/R^{0.5}$), that should be a constant value [16]. The average of the quantity varies depending on the catalog. These are between 4 and 6 $\mathrm{km\,s^{-1}\,pc^{-0.5}}$. Even so, data mostly oscillate in a range of 0.5 - 12.5 $\mathrm{km\,s^{-1}\,pc^{-0.5}}$ showing a considerable dispersion of median values.

We compiled information from the literature that include larger spatial scales (similar to the scales studied by Larson). Figure 5 shows the velocity dispersion-size relation for these literature catalogs (whose β coefficients are also shown in Table I) and our catalog of ^{13}CO. We can see a tendency of the data to follow the Solomon's relation (shown as a black line). The most consistent works with that relation are Rice's one, with a parameter of β = 0.53 studying 1064 massive molecular clouds [4] and Duarte-Cabral's, with β = 0.52 analysing 6664 sources

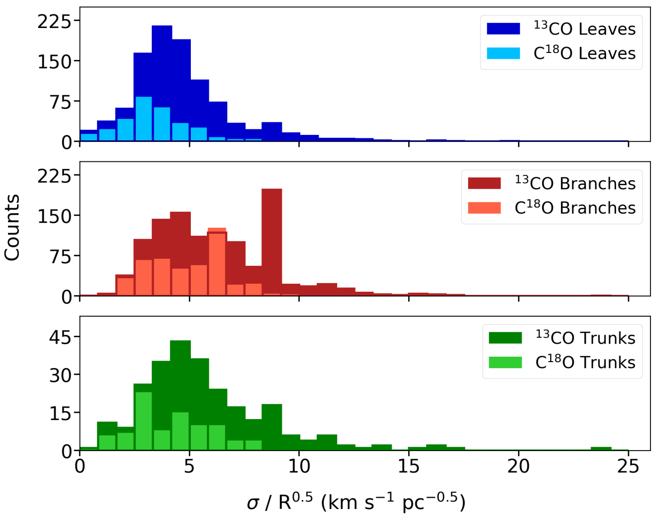

FIG. 4: Histograms of the leaves (blue), the branches (red) and the trunks (green) of first Larson's law for ^{13}CO and $C^{18}O$.

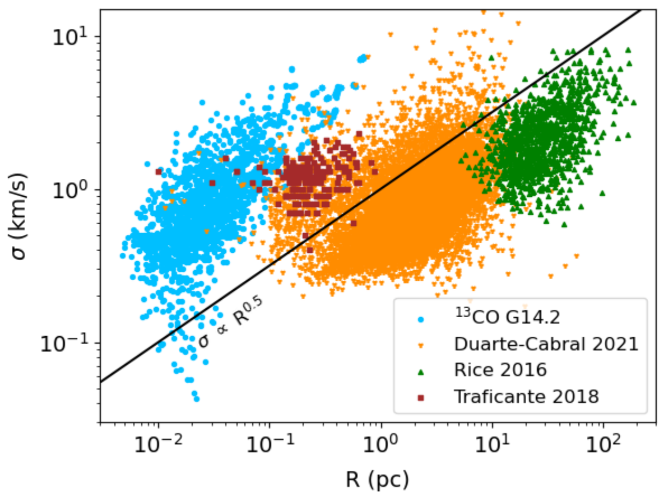

FIG. 5: Comparison of the velocity dispersion-size relation of the ^{13}CO in G14.2 (blue points) with other works from the literature.

TABLE I: Number of structures, relating coefficient of velocity dispersion-size and correlation coefficient of each catalog.

Catalog	**Structures**	β	R^2
$C^{18}O$ total	764	0.71 ± 0.02	0.73
$C^{18}O$ leaves	302	0.22 ± 0.08	0.03
$C^{18}O$ branches	462	0.69 ± 0.02	0.78
$C^{18}O$ trunks	88	0.65 ± 0.08	0.44
^{13}CO total	2122	0.66 ± 0.01	0.75
^{13}CO leaves	1002	0.32 ± 0.04	0.07
^{13}CO branches	1120	0.66 ± 0.01	0.78
^{13}CO trunks	258	0.60 ± 0.05	0.34
Rice 2016	1064	0.53 ± 0.03	-
Traficante 2018	213	0.09 ± 0.04	-
Duarte-Cabral 2021	6664	0.52	-

[17]. However, in Traficante's project the authors studied 213 massive clumps (i.e., lower scale structures compared to the previous works). The fit presents a smaller coefficient than the other studies (0.09) and the correlation between the magnitudes is very weak [16]. This is consistent with the low correlation coefficients we found for leaves' catalogs of G14.2.

These results suggest that at small scale sizes non-thermal motions are not dominated by interstellar turbulence but by other physical process that should be investigated.

IV. CONCLUSIONS

In this work we studied the rotational lines of $C^{18}O$ (1–0) and ^{13}CO (1–0) of the southern region of the IRDC G14.2. The goal was to analyse the first law of Larson in substructures of this molecular cloud using dendrograms. The main conclusions are:

- The morphology of both $C^{18}O$ and ^{13}CO is highly complex and filamentary.
- Generating dendrogram we identified 1061 structures in $C^{18}O$ and 2564 in ^{13}CO and obtained their velocity dispersion and size.
- There is a relation between velocity dispersion and size for the largest structures. The coefficients obtained are $\beta = 0.71$, $R^2 = 0.73$ for $C^{18}O$ and $\beta = 0.65$, $R^2 = 0.75$ for ^{13}CO. Although the correlation is large, the β coefficient don't match with Larson's first law.
- For the smaller structures we found a considerable number of points not adjusting to the regression. Also we found a very weak correlation ($R^2 = 0.03$ and $R^2 = 0.07$) between the studied magnitudes for the leaves. These information suggest that the model is not applicable to this scale order.

For future research it would be convenient to explore alternative methods for studying Larson's laws. This could include employing more sophisticated structure detection systems or observing denser molecules such as NH_3. These methods could offer a more thorough understanding and improve the precision of our results.

Acknowledgments

I would like to thank my advisor Dra. Gemma Busquet for her instruction and the guidance through this project. I also want to thank my parents, my boyfriend and my friends for their support.

[1] Estalella, R. and Anglada, G. (2008). "Introducción a la física del medio interestelar". Publicacions i Edicions de la Universitat de Barcelona. Textos docents; 50.
[2] Larson, R. (1981). "Turbulence and star formation in the molecular clouds". MNRAS. **194**. 809.
[3] Solomon, P. et al. (1998). "Mass, luminosity, and line width relations of Galactic molecular clouds". ApJ. **319**. 730.
[4] Rice, T. et al. (2016). "A Uniform Catalog of Molecular Clouds in the Milky Way". ApJ. **822**. 52.
[5] Elmegreen, B. and Lada, C. (1976). "Discovery of an extended (85 pc) molecular cloud associated with the M17 star-forming complex". ApJ. **81**. 1089.
[6] Gaia Collaboration (Brown, A. et al. 2018). "Gaia Data Release 2. Summary of the contents and survey properties". A&A. **616**. A1
[7] Zucker, C. et al. (2020). "A compendium of distances to molecular clouds in the Star Formation Handbook". A&A. **633**. A51.
[8] Busquet, G. et al. (2013). "Unveiling a Network of Parallel Filaments in the Infrared Dark Cloud G14.225-0.506". ApJL. **764**. L26.
[9] "Atacama Large Millimeter/submillimeter Array (ALMA)". `https://www.almaobservatory.org`
[10] "The Cologne Database for Molecular Spectroscopy (CDMS)". `https://cdms.astro.uni-koeln.de`
[11] "Common Astronomy Software Applications (CASA)". `https://casa.nrao.edu/`
[12] Rosolowsky, E. et al. (2008). "Structural Analysis of Molecular Clouds: Dendrograms". ApJ. **679**. 1338.
[13] "Astronomical Dendrograms in Python (`astrodendro`)". `http://www.dendrograms.org/`
[14] Chen, H. et al. (2019). "Filamentary Accretion Flows in the Infrared Dark Cloud G14.225–0.506 Revealed by ALMA". ApJ. **875**. 24.
[15] Caselli, P. and Myers, P. (1995). "The Line Width–Size Relation in Massive Cloud Cores". ApJ. **446**. 665.
[16] Traficante, A. et al. (2018). "Testing the Larson relations in massive clumps". MNRAS. **477**. 2220.
[17] Duarte-Cabral, A. et al. (2021). "The SEDIGISM survey: molecular clouds in the inner Galaxy". MNRAS. **500**(3). 3027.